Journal of Theoretical Biology 502 (2020) 110376

Contents lists available at ScienceDirect

Journal of Theoretical Biology

journal homepage: www.elsevier.com/locate/yjtbi

Assessing the impact of HIV treatment interruptions using stochastic cellular Automata

Andreas Hillmann *, Martin Crane, Heather J. Ruskin

Advanced Research Computing Centre for Complex Systems Modelling, School of Computing, Dublin City University, Dublin, Ireland

ARTICLE INFO

Article history:
Received 30 September 2019
Revised 23 April 2020
Accepted 12 June 2020
Available online 20 June 2020

Keywords:
Cellular automata
Modeling
Tissue
Disease
Treatment interruption

ABSTRACT

Chronic HIV infection causes a progressive decrease in the ability to maintain homeostasis resulting, after some time, in eventual break down of immune functions. Recent clinical research has shed light on a significant contribution of the lymphatic tissues, where HIV causes accumulation of collagen, (fibrosis). Specifically, where tissue is populated by certain types of functional stromal cells designated Fibroblastic Reticular Cells (FRCs), these have been found to play a crucial role in balancing out apoptosis and regeneration of naïve T-cells through 2-way cellular signaling. Tissue fibrosis not only impedes this signaling, effectively reducing T-cell levels through increased apoptosis of cells of both T- and FRC type but has been found to be *irreversible* by current HIV standard treatment (cART). While the therapy aims to block the viral lifecycle, cART-associated increase of T-cell levels in blood appears to conceal existing FRC impairment through fibrosis. This hidden impairment can lead to adverse consequences if treatment is interrupted, e.g. due to poor adherence (missing doses) or through periods recovering from drug toxicities. Formal clinical studies on treatment interruption have indicated possible adverse effects, but quantification of those effects in relation to interruption protocol and patient predisposition remains unclear. Accordingly, the impact of treatment interruption on lymphatic tissue structure and T-cell levels is explored here by means of computer simulation. A novel Stochastic Cellular Automata model is proposed, which utilizes all sources of clinical detail available to us (though sparse in part) for model parametrization. Sources are explicitly referenced and conflicting evidence from previous studies explored. The main focus is on (i) spatial aspects of collagen build up, together with (ii) collagen increase after repeated treatment interruptions to explore the dynamics of HIV-induced fibrosis and T-cell loss.

1. Introduction

While the importance of lymphatic tissues in HIV pathogenesis has long been known, (Fauci et al., 1996), research has focused mainly on their limited permeability to antiretroviral drugs and role as a viral reservoir, (Spiegel et al., 1992; Pantaleo et al., 1993). Recently, however dependency of immune system function on the structural integrity of *lymph tissue,* (Schacker et al., 2005; Zeng et al., 2011) has been suggested. Other factors, such as accumulation of highly differentiated T-cells, (with associated reduction of naïve variants), and the exhaustion of hematopoietic stem cells, are also assumed to be associated with HIV-induced degeneration and have been described extensively (see (Appay and Sauce, 2017) for a Review). In the following, therefore, the investigation focuses on the contribution of the tissue integrity to the immune system function and consequences of impairment for T-cell survival.

Specific cells, known as *Fibroblastic Reticular Cells* (FRCs), are present in T-cell zones of lymph nodes, (Fletcher et al., 2015), where they are associated with collagen fibers in a dense network (FRCn). Ongoing HIV infection causes changes in the levels of cytokines responsible for cellular signaling. For example, Transforming Growth Factor β1 (TGF-β1), has been found to be elevated in lymphatic tissue, (Theron et al., 2017) possibly expressed by increased numbers of Regulatory T-cells (TREGs), (Hasenkrug et al., 2018). The presence of TGF-β1 causes stromal cells to produce *additional collagen* leading to a low-level process of fibrosis in the T-cell zone, (Zeng et al., 2011). The resulting overgrowth, of the FRCn by collagen, causes these cells to block cellular signaling, (Fletcher et al., 2015). However, FRCs maintain a complex balance with CD4 + cells, ensuring homeostasis by exchange of cytokines and preventing apoptosis of both types of cell. Disruption of cellular signaling thus starts a vicious cycle of increased apoptosis of both CD4 + cells and FRCs. Rates of apoptosis have

* Corresponding author.
E-mail address: andreas.hillmann2@mail.dcu.ie (A. Hillmann).

https://doi.org/10.1016/j.jtbi.2020.110376
0022-5193/

been found to be strongly correlated with the *area of the collagenated region*, (Zeng et al., 2012). Administration of state-of-art *combination Antiretroviral Therapy* (cART) effectively blocks key pathways of the viral lifecycle thus reducing CD4 + cell loss due to viral activity, (Günthard etal., 2014). Levels of CD4 + cells have been found to rise subsequently with consequent normalizing of cytokine levels, (Kassutto et al., 2006), slowing down the tissue collagenation process leading to recovery of FRC levels, (Zeng et al., 2012). However, cART can not undo *existing fibrosis*, (Zeng et al., 2012), with this resulting in permanent but hidden immune system impairment which may influence disease progression and subsequent response to treatment when treatment is reinstated after an interruption. Administration of antifibrotic agents has been *successfully* tested in an *SIV context*, (Estes et al., 2015) but we have not been able to find corresponding clinical studies in humans. The overall process of collagenation has been researched in some detail, but spatial aspects of collagenation patterns and their effects remains unclear. Although 'black holes' in the FRCn, (with an absence of functional FRCs), have been found to be associated with lower CD4 + concentrations and higher rates of apoptosis, (Zeng et al., 2011), the impact of spatial heterogeneity over affected tissue as a whole has yet to be investigated.

Interruptions of cART are still common, despite contrary recommendation by medical authorities, (WHO, Consolidated guidelines on the use of antiretroviral drugs for treating and preventing HIV infection, 2013). The demands of daily lifelong medication associated with cART have long been known to engender both physiological and psychological problems such as drug toxicity effects, (Masenyetse et al., 2015) and drug fatigue, (Pai and Lawrence, 2006) respectively. These factors frequently engender *non-adherence* (missing drug dose voluntarily or otherwise), (Glass and Cavassini, 2014), or so-called 'drug holidays' (interruption of treatment for an extended period without authorization), (Wakode, 2013). In certain resource-limited settings, interruptions may also result from insufficient amounts of antiretroviral drugs, (Mann et al., 2013), lack of knowledge, on requirements for ongoing treatment or pharmacodynamics of the active agent, (Nozaki et al., 2013), or from fear of stigma, (Murray et al., 2009). Treatment discontinuation leads to *viral rebound*, a rapid increase of viral particles which become detectable in blood after about 10 days, (Rothenberger et al., 2015). Few clinical studies have studied, in a structured way, the effects of treatment interruptions over longer timescales, (Benson, 2006). Conventionally, such Structured Treatment Interruptions (STIs) were regarded either as a means to reduce drug toxicity, reduce costs and potentially allow immune functions to recover, (Rosenberg et al., 2000) or as a way to achieve removal of drug resistant virus by outgrowth of wild type, (Brenner et al., 2002). Study results on impact have been variable: one study noted increased fatalities, (El-Sadr et al., 2006), while no detrimental effects were found compared to continuous treatment in others, (Maggiolo et al., 2009); some adverse effects such as drug resistant mutations were also reported, (García et al., 2001), while beneficial effects on immune control were observed in exceptional cases only, (Rosenberg et al., 2000). To date, treatment interruptions are not recommended by medical experts, whereas an early start to treatment and indefinite administration are advocated. Nevertheless, conflicting outcomes of different clinical studies offer no clear indication on the circumstances under which treatment interruptions might pose a 'clinically acceptable' risk given that unstructured interruptions can also occur in reality.

However, while cART (with associated drug burden) remains the only effective means to counteract HIV-infection, (unstructured) treatment interruptions seem inevitable. Assessing potentially harmful outcomes is therefore of vital importance and, where clinical data are out of reach, *in-silico* approaches aims to provide insights into past study outcomes as well as guidance for future clinical study, (Bueno-Orovio et al., 2017). In the context of HIV, a particularly rich base of models (predominantly based on *Ordinary Differential Equations*) has existed since the early 1990s and has been used to explore a number of disease aspects (Perelson and Nelson, 1999). However, due to the core assumption of a 'well-mixed' environment, their use for the analysis of treatment interruptions is limited since spatial heterogeneity, now thought to be important, (Hillmann et al., 2017), is not accommodated.

In consequence, computational or stochastic approaches have gained traction in recent years, utilizing growing availability of cost-efficient computing power and modifying ODE-based results. A noteworthy example is C-IMMSIM, (Bernaschi and Castiglione, 2001), serving as an agent-based framework for cellular components of the immune system to simulate aspects of the its response, such as antigen recognition and T-cell maturation. The latter is modelled following an elaborate approach with receptors represented by bit-strings (first reported (Celada and Seiden, 1992). The framework was subsequently also used to assess HIV treatment initiation timing, (Paci et al., 2011), and interruptions, (Castiglione et al., 2007; Mancini et al., 2012). While C-IMMSIMM serves well as a general-purpose immune system simulator, some limitations for application to HIV treatment interruptions apply. The framework is designed to focus on aspects of immune surveillance evasion through viral mutation and latent infection of T-cells, (Mancini et al., 2012), so aims to explain immune failure after interruptions in a similar fashion to that of older ODE models. However, other key aspects, such as drug resistance and tissue dynamics, are not considered. It is difficult to obtain sufficiently exact parameters due to the high level of computational complexity for core functions, (Castiglione and Celada, 2015) while the model has high computational cost with heavy demand on computational resources, (Halling-Brown et al., 2010). Further, while the framework is detailed and complex in some respects, omission of key aspects (as noted above), suggest that diverse implications of treatment interruptions are not explored. Any model represents a compromise between realism, feasibility and availability of relevant data for computation. The contention is that a more specific model, with sufficient level of detail to investigate the lymphatic tissue domain, is indicated, and is the focus of work presented here.

Few mathematical or computational models have been proposed to describe processes, inherent to lymphatic tissue, with most approaches focusing on the role of the network as the structural element of T-cell trafficking, (Beltman et al., 2007; Linderman et al., 2010; Bogle and Dunbar, 2010; Graw and Regoes, 2012; Donovan and Lythe, 2012). More recently, the function of the FRCn in the context of immune response has been considered, (Textor et al., 2016) and a detailed representation of the microscopic network structure proposed (Savinkov et al., 2017). However, only a limited number of models have addressed the issue of HIV-induced alterations of the tissue matrix. In a recent study, Donovan and Lythe, (Donovan and Lythe, 2016), constructed a PDE model to assess the impact of collagenation of the FRCn on CD4 + concentration recovery after treatment initiation. The model focused on aspects of CD4 + proliferation and excluded spatial effects by assuming that all 'reagents' were distributed uniformly over model space. The authors argue that a spatial representation, such as an Agent Based Model, is computationally costly and spatial effects negligible due to (near) random movement of CD4 + cells.

Nonetheless, spatial aspects have been found to play a *major role* in many areas of HIV infection, (Graw et al., 2013), with data suggesting impact on the FRCn as well. As noted earlier, functional CD4 + cells have been found to be located predominantly in intact regions of the FRCn while apoptotic cells were co-located with high-collagen regions, (Zeng et al., 2011). Also, despite

CD4 + cells appearing to traverse the FRCn in a near random fashion, (Linderman et al., 2010), cells enter the lymph node through *dedicated conduits* termed high endothelial venules (HEVs), (Ager and May 2015), suggesting that distribution of CD4 + cells over the network is non-uniform. Though molecular mechanisms of collagen formation are mostly well-known, (Zeng et al., 2012), spatial formation patterns have yet to be obtained. The main mechanism appears to be connected with the elongation of existing collagen fibers, (Zeng et al., 2012) which may argue for distinctive spatial formation patterns.

We address these lacunae arising from previous work in the following way: (i) In assessing effects of FRCn degradation due to HIV infection, a model framework is proposed which includes spatial heterogeneity aspects of the lymphatic microenvironment rather than the traditional assumption of a well-mixed situation; (ii) this specific adaptation permits focus on mechanisms important to collagen formation patterns, so that computational cost is modest compared to adaptation of a large-scale model, which includes features of less immediate interest.

2. Methods

Cellular Automata (CA) approaches (Beauchemin et al., 2006; Escobar Ospina and Perdomo, 2013; González et al., 2013), have become popular for quantitative assessment of disease effects on immune system function, (Chavali et al., 2008). This material presented here builds on (Hillmann et al., 2017), in order to illustrate a heterogenous distribution of CD4 + cells (assumed homogenous with the original approach). As with (Hillmann et al., 2017), the lattice represents a fraction of the FRCn of a lymph node, with sites in either a healthy or impaired state. Each site of the CA is assumed to represent one FRC, directly connected to its n nearest neighbors. This assumption is in line with clinical data, suggesting a lattice-like topology of the FRCn with small-world features, (Novkovic et al., 2016). These latter enable (additional) connections to more distant sites, allowing for *non-local* (as opposed to neighborhood) effects. In CA terms, these small-world properties are achieved by assigning states to a given fraction of randomly selected sites with state changes obtained through neighborhood-effects, (Yang and Yang, 2007).

For CD4 + motility, we adopt the assumption of a random walk suggested by microscopic data, (von Andrian and Mempel, 2003). Thus, we have a reasonable basis to assume that CD4 + cells enter the simulated lymphatic network only at HEVs, (Ager and May 2015) and perform a random walk over simulated FRCn from these conduit sites. It is worth noting that T-cells may also enter lymph nodes via other routes (e.g. afferent lymphatics). However, the quantities of T-cells migrating through such routes in relation to HEVs are not sufficiently known. One possibility is that the process may be regarded as a baseline reduction of CD4 + cells, independent of spatial considerations such as those we explore here for collagenation.

The model time step was set to represent a week in real time to enable assessment of both mid- and long-term-effects. Our model considers the spatial effects of collagen formation and depletion of CD4 + cells. This reduction in cell numbers is due either to direct viral effects or to collagenation of the lymphatic tissue matrix where, under ART administration, the former is *reversible* but not the latter.

To account for the marked computational cost required to track a large number of separate CD4 + cells passing through lymphatic tissue, we generate a probability distribution for a given cell being present at any lattice site. The cellular automata model was implemented in the C++ programming language with key features illustrated in Fig. 1, with separate elements and their rationale described in more detail as follows.

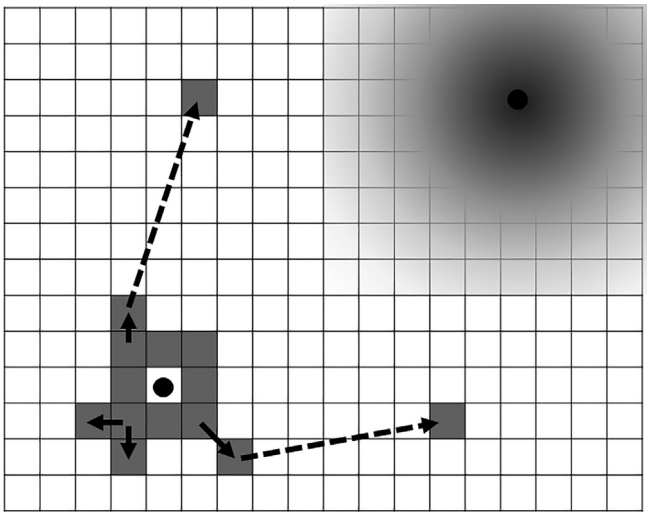

Fig. 1. Fundamental concepts of on-lattice collagenation model. Left side: Solid arrows indicate neighborhood effects. Originating from HEVs (black dots), collagen (solid grey boxes) spreads to adjacent uncollagenated/healthy sites (white boxes). Right side: Probability of CD4 + cells found present (grey shading/overlay) decreases quadratically with distance to HEVs, based on current assumptions of slow movement. In the event of more rapid T-cell dispersion (or influx from other sources) probabilities close to HEV regions would be relatively low, which corresponds to a more uniform distribution.

2.1. Simulation environment

A 2-dimensional square lattice with each site representing a single FRC forms the basis of all simulations. The actual FRCn occupies a 3-dimensional space in the approximately spherical lymph node. Human lymph node sizes span a range between 0.5 and 2 cm, (Ward et al., 2018). Diameters larger than 1.5 cm are in the short axis are usually considered pathological, (Ganeshalingam and Koh, 2009; van den Brekel et al., 1998). For our study, we assume an average diameter of ~1 cm, acknowledging that other sizes in the above-mentioned range are possible. Microscopic imaging data on the FRCn has been obtained using histological cuts of the actual organ, e.g. Novkovic et al, (Novkovic et al., 2016), offering some insight into the 3-dimensional topology of the reticular network. Translating this data into an exact computational representation of the network structure along with different functional areas in a lymph node has been a focus of recent work, (Bocharov et al., 2015). However, to address broad questions of collagenation in context of HIV, simplifications can reasonably reduce complexity while retaining enough information about the system. In this context, reduction of dimensions is used to address the problem in a 'layered' fashion. and has been commonly employed in the context of investigating the spread of HIV in tissues, e.g. (González et al., 2013; Strain et al., 2002; Precharattana, 2016). Taking into account clinical literature to date, a 2D representation and parameter ranges can capture qualified tissue features on which to base further hypotheses.

The mean distance between the centers of reticular cells (FRCs) has been determined to be in the range of 21–30 μm, (Graw and Regoes, 2012), or in the order of 23 μm according to recent murine experiments, (Novkovic et al., 2018). In any case, a histologic section through the whole organ would correspond to a square lattice with side length of approximately 500. The vast majority of FRCs has been found to be connected to 6–11 (median 8) neighboring cells, (Novkovic et al., 2016), with a smaller number of FRCs of

higher connectivity responsible for the small-world characteristics of the network. To simulate small-world properties in our CA model, the neighborhood of a site (as for the classical Moore neighborhood) was taken to be the 8 nearest-neighbors for the majority of FRCs, while a site might also be connected to a randomly-selected site with a probability P_S, (Yang and Yang, 2007), (see model rule 2). For each lattice site, one of two states was assumed: *H* (healthy FRC, no collagen), and *C* (covered by collagen, no FRC). During model initialization, all sites of the 500x500 lattice were assigned a state *H*, with the exception of a random fraction P_{HEV} representing HEVs as entry points for CD4 + cells, with special state *CH*. The density of HEVs in the T-cell zone of a lymph node remains inconclusive and is apparently variable depending on immune system status, (Ager, 2017). Available data, however, indicate a density of about 18 per square millimeter, (Shen et al., 2014), which translates to an estimate of ~0.01 for P_{HEV}.

2.2. Tissue collagenation

State changes (or transitions) at lattice sites follow a probabilistic set of rules, where at unit time step *t*, change from state × to a state *y* is represented by a probability $P_{x\rightarrow y}$; (indices are assigned for clarity). While some transition probabilities have fixed values, others depend on the neighborhood of a given site.

Updates are performed in discrete time steps, where each step represents ~1 week in real-time. This choice of interval reflects the fact that collagenation occurs over years, i.e. is slow compared to other aspects of HIV infection (such as infected cell turnaround and corresponding immune response).

The model rules for collagenation spread are as follows, (designated by cell state type and mechanism).

1 Rule $H \rightarrow C$ (neighborhood-driven):
$P_{H\rightarrow C\ (N)} = (1-(1-P_{INF})^N)$
2 Rule $H \rightarrow C$ (random – small world):
$P_{H\rightarrow C\ (S)} = P_S$
3 Rule $C \rightarrow H$ (regeneration):
$P_{C\rightarrow H} = P_R = 0$

Description: Initially, collagenation is seeded by assigning state *CH* to random sites with probability P_{HEV} which serve as origins of collagenation while all other sites are assigned to state *H*.

1 The first rule expresses the chance that a given site may become collagenated, depending on the amount of collagen already present in the neighborhood, (as suggested by microscopic data), [13]. The collagenation process is ascribed to factors, such as presence of Transforming Growth Factor β1 (TGF-β1), [8] which is commonly excreted by regulatory T-cells (TREGs). The number of these cells is high during HIV infection, possibly related to inflammation processes, (Hasenkrug et al., 2018): TGF-β1 in the model here is taken to be a scalar represented by probability $P_{H\ \rightarrow\ C\ (N)}$ which depends on the number of collagenated neighbors and is thus non-uniform. *Each* of N collagenated neighbors of a site with state H may cause collagenation of a given site with a probability P_{INF} (of inflammation) at each time step: the contribution to $P_{H\rightarrow C\ (N)}$ is thus binomial. We assume that *N* may take values from 0 to 8, (*Moore* neighborhood), as above (Novkovic et al., 2016).
2 Given the evidence of the FRCn having small-world topology, (Novkovic et al., 2016), state changes can also be ascribed to neighborhood effects at random sites. Changes are triggered with probability dependent on the interconnection between different clusters, Yang and Yang (2007), where high values of interconnection lead to approximation by a random network. For random collagenation, therefore, our CA model mimics this process by introducing an alternative rule for H → C, where a site selected at random assumes state, *C*, with a probability P_S. This rule is applied at each iteration in addition to rule 1 and leads to an accumulation of collagen at random sites (in addition to local accumulation). However, use of this rule is confined to preliminary experiments (see results) to determine an estimate for P_S while considering only the special case of P_S = 0 for subsequent experiments to emphasize local collagenation.
3 Finally, we note that, while some clinical data do provide evidence of a small, albeit significant, FRC regeneration once antiretroviral treatment is initiated, (Zeng et al., 2012), the strong general evidence is that collagenation is irreversible. Regeneration is thus assigned a probability of zero in these preliminary numerical experiments.

2.3. T-cell Degradation

Collagenation progression is slow compared to traversal of CD4 + cells through the FRCn; a discrete probability is thus associated with random occupation of a given lattice site by a cell at each time step. Cell movement can be taken as random from entry points, as suggested by earlier modelling studies (Donovan and Lythe, 2012). Thus, the average distance of a cell from its entry point increases in a linear manner with the square root of time elapsed. Conversely, the distances of a large number of cells from their point of entry are assumed to be Normally distributed, follow a 2-dimensional Normal Distribution with discrete steps around the location of the HEVs as the mean. The Standard Deviation can then be validated from clinical data: Assuming an average cell movement time of 10 h within a lymph node and a diffusivity of 60 μm^2/minute, (Ganusov and Auerbach, 2014), with average path length of 23 μm, (Novkovic et al., 2016), a Standard Deviation of ~8.5 lattice sites from HEV locations is indicated. The resulting distributions ($P_1 \ldots P_n$) describe the probability of a lymphocyte being present around each of the n HEVs in the model. Conflating these n distributions yields the overall probability distribution *P(L)* of presence of a lymphocyte for any lattice location. The heat map in Fig. 2 illustrates this spatially heterogenous probability.

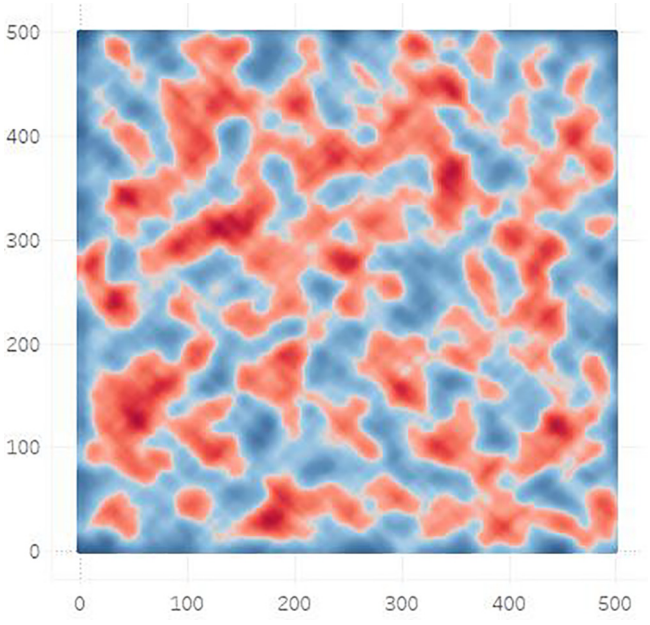

Fig. 2. A (500 × 500) lattice section for lymphatic tissue showing spatially heterogenous probabilities of CD4 + cell presence. Regions around HEVs (conduit entries for CD4 + cell movements; red) are associated with high probabilities, compared to non-HEV areas (blue). (For interpretation of the references to colour in this figure legend, the reader is referred to the web version of this article.)

We further state that an individual CD4 cell has a probability *P(AP|L)* of undergoing apoptosis when close to a collagenated site. A link between terminal tissue fibrosis and AIDS disease has been suggested, where AIDS is associated with an approximate reduction of 80% or more of CD4 + cells from baseline, (Fauci et al., 1996). This means that when collagenation spans the whole T-cell zone – which is the case for the AIDS stage – CD4 + cells are reduced to about 20% of the amount found in a healthy state. In consequence, an approximate value of 0.8 is initially chosen for *P(AP|L)*. Due to patient-specific variations of the amount of CD4 + cell decline until AIDS emerges, other values within the range (0.7, 1.0) are also possible.

According to Bayes Theorem, the overall probability distribution *P(AP)* for apoptosis of a CD4 + cell at any lattice site is obtained by the relation:

$$P(AP) = \frac{P(AP|L)P(L)}{P(L|AP)} \tag{1}$$

Apoptosis may only occur for a site with Lymphocytes present, hence *P(L|AP)* becomes unity and *P(AP)* can be calculated by the simple product of *P(AP|L)* and *P(L)*. The resulting spatially dependent probability distribution for apoptosis is computed for every time step.

2.4. Parameter estimates

Parameter estimates, as described above, are summarized in Table 1, with clinical data sources cited. Obtaining estimates for P_{INF} and P_S which control collagenation progression in the model is challenging due to the difficulty of obtaining lymph tissue samples over the time course of HIV infection. A pool of patients was studied by Zeng et al. (2012) with individuals assigned to one of three disease stages of HIV infection based (healthy, pre-symptomatic, AIDS) based on their CD4 + counts. The patients who did not receive antiretroviral treatment prior to the study were subject to lymph node biopsies, where analysis gave rise to quantification of FRCn and collagen. The procedure was repeated some months after patients started Antiretroviral Therapy. A remarkable result was the collagen accumulations remaining constant after months of treatment, while FRCn levels recovered at a certain degree. These classifications provide coarse guidance on progression of collagenation with time, but since the asymptomatic phase of HIV infection can last for 10 years, granularity is low.

However, the amount of collagenation over a period of time has been found to be inversely correlated with CD4 + cell count in lymphatic tissue, (Estes, 2013), similar to findings for blood. In consequence, we utilize clinical data on progression of CD4 + counts in blood (Fauci et al., 1996), where these show linear decline. Assuming a similar relation for lymphatic tissue in our model, a decrease of 0.19% of baseline CD4 + cells per week is assumed when no treatment is applied. This value is based on the observation that CD4 + depletion develops gradually from beginning of the chronic phase of HIV infection which takes ~10 years (in absence of treatment) until AIDS symptoms emerge. It is should be noted, however, that this rate presents a typical value based on population average. A period as short as 3 years to AIDS symptoms ('fast progressors') has been observed, (Ruffault et al., 1995), up to decades without visual depletion ('elite controllers'). It should be noted, however, that such cases (specifically the latter) are extremely rare. A more detailed exploration of these extreme values must motivate future sensitivity analysis.

Table 1
Parameter estimates for the spatial CA Tissue Model (from the literature).

Parameter name	Parameter value (range)	Source
P_{HEV}	0.01 (0.006; 0.016)	Shen et al. (2014)
P_R	0 (−6.3E−3; 7.7E−03)	Zeng et al. (2012)
P(L)	N ~ 0, 8.5	Ganusov and Auerbach (2014)
P(AP|L)	0.8 (1.0; 0.65)	Fauci et al. (1996)
Square Lattice side length	500 ± (250; 1000)	Novkovic et al. (2018)
Neighborhood size	8 (7.91; 8.558)	Novkovic et al. (2016)

2.5. Simulation setup

Our primary aim is to assess the contribution of spatial effects on the overall decrease of CD4 + cells through lymph tissue collagenation and the related FRC loss. In this context, it is interesting to observe differences in the overall result if spatial effects are cancelled out, i.e. if collagenation is allowed to take place exclusively due to random effects. In the latter case, only random collagen growth is permitted i.e. lattice cells may change their state from *H* to *C* with a fixed probability P_{rand} at each time step (termed 'random model' in the following). To determine spatial contribution, we assign amount of collagen in the context of apoptosis risk, (used as a measure for CD4 + survival) by implementing computer simulations for the two models (spatial/random model), highlighted above.

In this context, specific parameter estimates (P_{INF}, P_S, P_{rand}) can not be obtained directly from the literature, so required implementation of an inverse Monte Carlo approach, (McGreevy, 2001). This enabled exploration of the parameter spaces of the respective models (the 'spatial' or localized/small world and random versions). Repeated sampling is used to find *candidate parameter combinations* which are scored on the basis of closeness of the simulated CD4 + apoptosis rates to CD4 + decline rates from clinical data, using a Root Mean Square Error (RMSE) measure. CD4 + cell loss shows great patient-specific variability with AIDS symptoms emerging from three years to decades post infection, (e.g. (Okoye and Picker, 2013). For this study, we use a population average obtained from (Fauci et al., 1996; Greenough et al., 1999), indicating a constant CD4 + cell loss of 0.19% per week from baseline (zero order). Depending on the score change at each iteration the candidate parameter refinement is either accepted (and used as the new basis for sampling) or rejected. To avoid the problem of convergence at local minima, this 'hill-climbing' algorithm also employed a typical Metropolis-Hastings, (Robert, 2015) modification.

Finally, in order to show the contribution of spatial heterogeneity to CD4 + count decrease during antiretroviral treatment interruptions, treatment initiation was mimicked by effectively stopping simulated collagenation (setting respective probabilities to zero) at different simulated infection stages, then subsequently interrupted for fixed time periods.

3. Results and discussion

I. Spatial aspects of collagen formation have been found to be associated with CD4 + apoptosis rates. For calibration of the spatial model 5000 inverse Monte Carlo steps were performed in total, with different starting values for P_{INF} and P_S chosen at random every 1000 steps. Fig. 3 shows results for a subset of the generated data, namely the 1000 points with near-optimal scores, where candidate values of the parameter describing neighborhood effects P_{INF} are plotted against their score function (RMS). The curve indicates a minimum RMS around values of P_{INF} between 0.0015 and 0.0045 depending on the setting of the 'small world' parameter P_S chosen. We found P_{INF} and P_S to be correlated in a power law fashion as

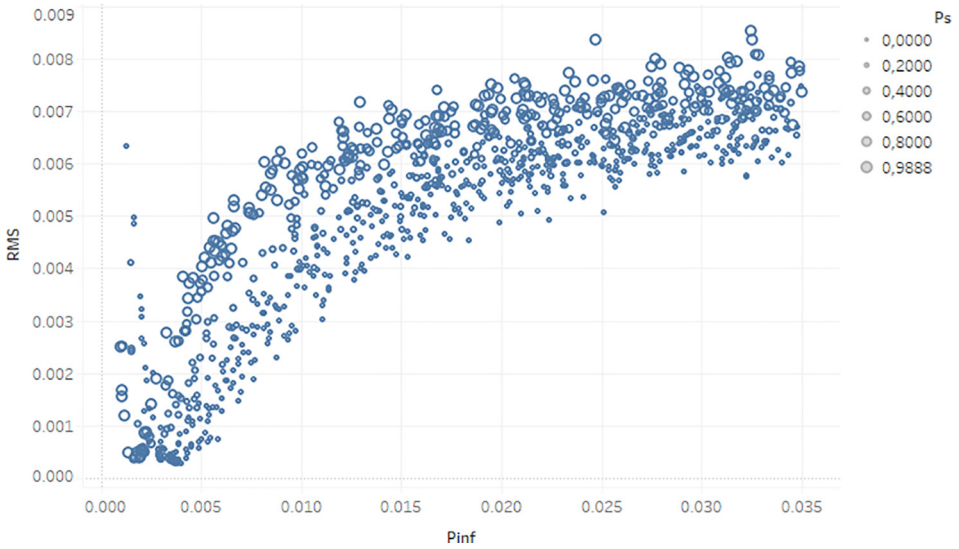

Fig. 3. Result of 1000 inverse MC steps for the spatial model. The X-axis denotes possible values for spatial collagenation parameter P_{INF} while the Y-axis corresponds to RMSE w.r.t. clinical data match. Marker sizes indicate value of corresponding 'small world' parameter P_S.

suggested, (Yang and Yang, 2007), with $P_{INF} = 0.0021 * P_S^{-0.195}$ in this case. While linking these directly to clinical outcome is tentative, however, due to insufficient data about the degree of small world in lymph tissue, the potential for refinement is clear. Given the availability of more detailed data, it should be possible to narrow down the range of possible values for P_{INF} and P_S, which would in turn provide a more exact representation of FRCn structure in the CA model with corresponding improved viability of simulation outcomes. As noted above, we assume the special case of P_S to be zero for subsequent spatial model simulations since our emphasis is on local collagenation patterns. The random model with one parameter was calibrated using 1000 Monte Carlo steps, where a clearly defined minimum in terms of RMSE could be identified at $P_{rand} \sim \underset{\sim}{\updownarrow} 0.0035$ (see Fig. 4).

To account for the heterogeneous progression rates of untreated HIV infection observed in clinical practice, we varied the CD4 + decline rates used for model calibration, using known extreme values in both directions. Hence, to account for *fast progressors* we used a decline rate twice as high as the average case. Conversely, we used a decline rate half the normal rate to account for *long term (non–) progressors*. Estimated data for P_{INF} and P_{rand} obtained by inverse MC simulations for a range of progression speeds are presented in Table 2. Such a sensitivity analysis is useful to test model robustness and to determine valid parameter ranges. Results indicate clearly-defined parameter ranges for P_{INF} and P_{rand}; however, for steeper slopes of CD4 + decline (as for fast progressors) the range of possible parameter values is wider, (i.e. is less precise). Also, both parameters appear to change proportionally with progression speed. Doubling or halving progression speed is reflected in similar proportional changes in P_{INF}, while the factor for P_{rand} is around three.

The different dynamics for random and spatial model are illustrated in Fig. 5. Both panels show collagenation patterns for 100 time steps (~2 years) after simulated infection for a similar degree

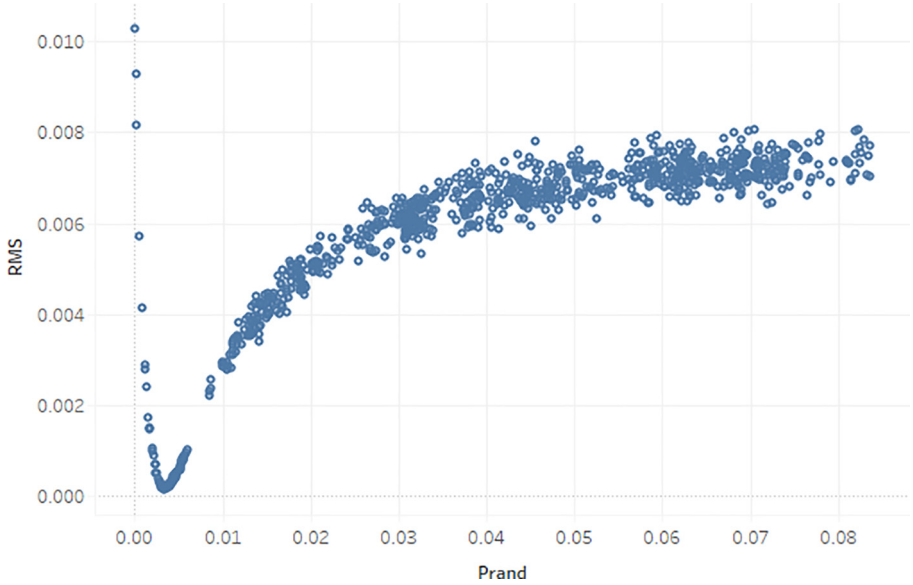

Fig. 4. Result of 1000 inverse MC steps for the random model. The X-axis denotes possible values for random collagenation parameter P_{rand} while the Y-axis corresponds to RMSE w.r.t. clinical data match. Minimum RMSE value is obtained for $P_{rand} \sim 0.0035$.

Table 2
Estimates for Pinf and Prand obtained by inverse MC simulations in relation to different infection progression speeds. Values denote averages and standard deviations of the 50 lowest scoring MC samples.

Parameter	Infection progression (years until CD4 + depletion)		
	Fast (5 years)	*Average (10 years)*	*Slow (20 years)*
P_{INF}	0.0093 (0.0011)	0.0042 (0.0028)	0.0024 (0.00024)
P_{rand}	0.011 (0.0027)	0.0035 (0.00070)	0.0012 (0.00028)

of CD4 + apoptosis. For the spatial model (Fig. 5a) it is clear that collagen is concentrated in *specific regions* (colored red), predominantly around HEVs where CD4 + cells have a high probability of being present, whereas for the random model (Fig. 5b), collagen is more diffused (colored blue) over the simulated tissue. The consequences of those differences in collagen clustering on CD4 + apoptosis are illustrated in Fig. 6. The ratio of the total reduction of CD4 + cells due to collagenation to total collagen accumulation is defined here as 'relative apoptosis'.

Since collagen formation starts at sites with high CD4 + throughput (HEVs) for the spatial model (Fig. 6a), relative apoptosis starts high but reaches a plateau over time as collagenation spreads to regions with fewer CD4 + cells. In contrast, relative apoptosis remains constant for the random model since collagen appears at random locations, irrespective of CD4 + cell occupation. Thus, for total collagen percentage over time, as shown in Fig. 6b, curve

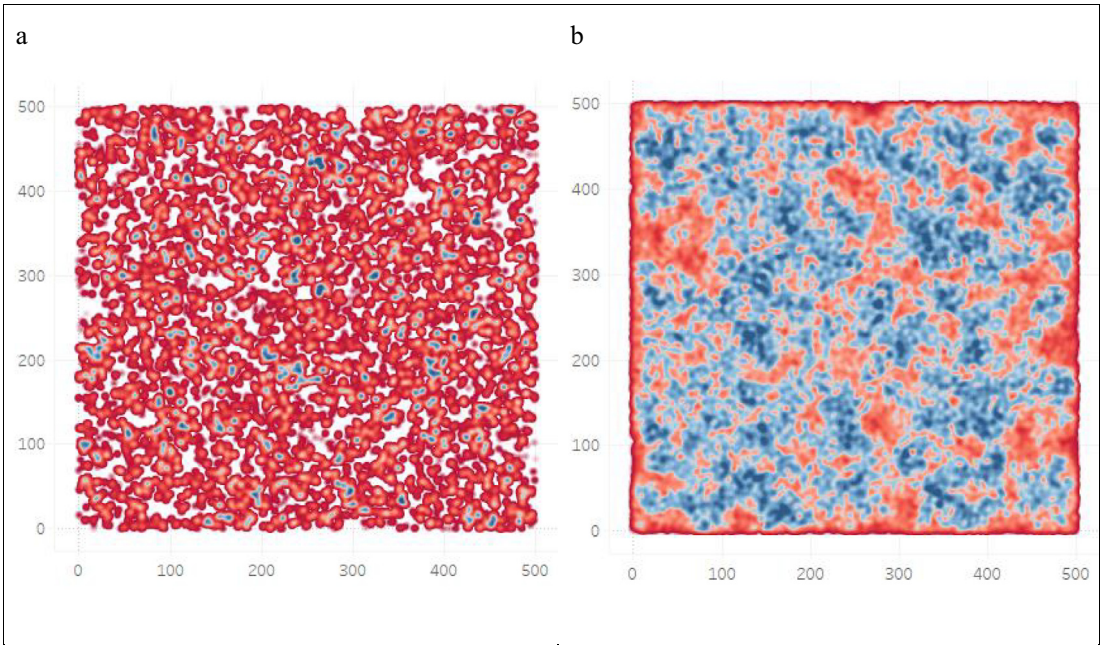

Fig. 5. Lattice snapshots of simulated collagen localization for spatial model (a) and random model (b), at simulation time step 100 (equivalent to ~ 2 years). Collagenation forms more distinct clusters (a) compared to (b). Colors indicate simulated collagen density (red – high; blue – low; white - none). (For interpretation of the references to colour in this figure legend, the reader is referred to the web version of this article.)

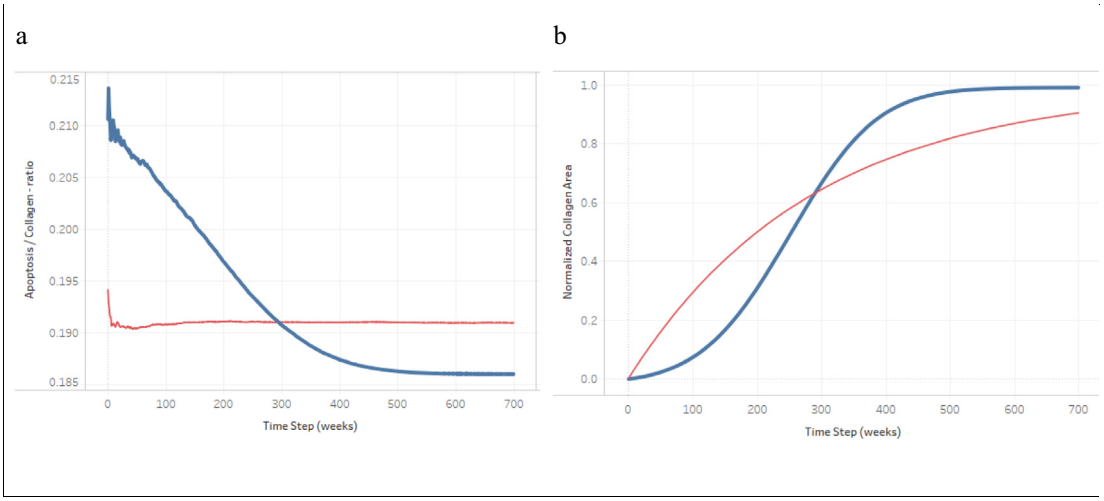

Fig. 6. Apoptosis rates per collagenated area (a) and profiles of collagen growth over time (b) for the spatial model (thick blue line) and random model (thin red line). Y axis denotes ratio between the total reduction of CD4 + cells due to collagenation and total collagen accumulation. (Parameters. spatial model: $P_{INF} = 0.035$, $P_S = 0$; random model: $P_{rand} = 0.0035$, Y-scale in (a) truncated for visibility). (For interpretation of the references to colour in this figure legend, the reader is referred to the web version of this article.)

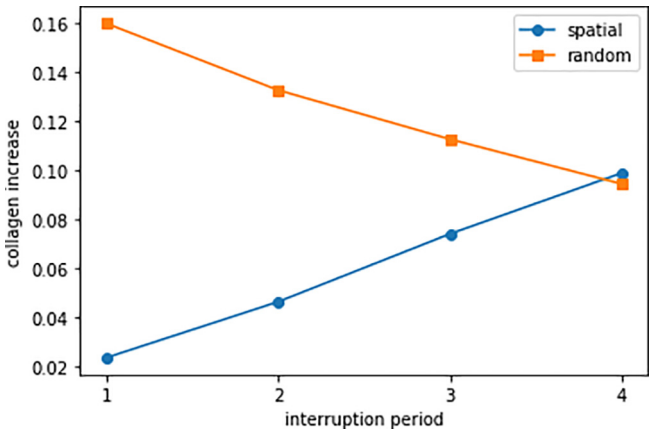

Fig. 7. Differences in collagenation increase following interruptions depend on amount of pre-existing collagenation for spatial (blue circles) and random model (orange squares). Markers denote total increase from baseline in collagenation (Y-axis) during subsequent interruption periods (X-axis). Extended treatment interruptions between time steps (weeks) 50, 150, 250, 350 with respective duration of 50 time steps. (For interpretation of the references to colour in this figure legend, the reader is referred to the web version of this article.)

shapes are markedly different. Despite constant decay of CD4 + cells (zero order), neither curve is linear, suggesting that exact mechanisms of collagen formation patterns are yet to be completely identified. Nevertheless, our results clearly show that both spatial and random models agree with clinical data in terms of showing CD4 + count decline. However, different predictions for the ratio of total CD4 + reduction and collagenated areas (relative apoptosis) are obtained, since collagenation is more marked in the spatial model. The fact that both models do not give the same results concerning collagen accumulation and CD4 + decline, might provide a connecting point for clinical research in assessing the impact of spatial collagenation patterns in greater detail.

II The *persistent* effects of treatment *interruptions* also appear to be related to treatment initiation timing or pre-existing immune damage, (Hillmann et al., 2017). Using either of our models, treatment interruption shows as an increase in collagenation, which is halted but *not reversed* after re-initiation. Detailed data for this sharp increase are displayed in Fig. 7 and illustrate the different behavior of both models in terms of collagen build up. Results indicate that the amount of interruption-induced *extra* collagenation *changes steadily* for repeated treatment interruption and re-initiation. However, the slope directions differ markedly among the two models. For the random model, collagen buildup occurs rapidly during the first interruptions but slows for subsequent interruptions. The spatial model exhibits an inverse slope, with the slow rate of collagenation for early treatment interruptions increasing for each subsequent interruption. This profile of rate change also indicates that large collagenated areas (present at later stages of infection) will inevitably spread more rapidly in the spatial model if treatment is removed, since the contact boundary with uncollagenated areas is also larger. The implications for treatment interruptions are particularly clear. While few interruptions are less deleterious for predominantly spatial collagen spread (and might be clinically acceptable under certain circumstances), random spread implies that a first interruption is associated with the most severe collagen increase and should be avoided.

4. Conclusion

In this study, we have addressed patterns of collagenation, arising from HIV infection under a set of assumptions for infection progression. The role of lymphatic tissue features in impairment of immune system homeostasis is of considerable interest, but clinical data are sparse to date, (Zeng et al., 2011). The best detailed knowledge from recent clinical studies on indicative features is used to indicate plausible ranges for key parameters and properties of the prototype network assessed, using a CA approach. Small world aspects have been considered in preliminary experiments, (for example aspects of CD4 + trafficking simplified as a random walk), but further elaboration of our basic models is feasible.

Results from the computer simulations indicate that collagen formation patterns do influence the overall apoptosis rate of CD4 + cells. Comparing our spatial model with random collagenation in neither case indicates that accumulation of collagen occurs at a constant (zero order) rate as suggested by clinical evidence of a linear decline of CD4 + cells and its connection to collagen deposits. For collagen increase directly reflecting the linear decline of CD4 + counts, we argue that a combination of both spatial and random effects is involved. Further investigation on viable parameter ranges and model modification is clearly indicated.

Our results further suggest that the amount of lymph tissue fibrosis caused by antiretroviral treatment interruptions depend on the frequency and length of these interruptions. Based on the preliminary assumptions adopted, we were able to quantify these minute increases in tissue fibrosis. Indications also are that spatial and/or random effects have marked impact on collagenation, with adverse effects dependent on which of these predominate and the number of interruptions which occur. Pre-existing collagen deposition may explain the variability in terms of T-cell loss and related events in reported clinical studies, following interruptions of antiretroviral treatment. Given that tissue effects were not considered in these studies, this may partially explain the conflicting findings (Hirschel and Flanigan, 2009).

One motivation for this study was to explore whether a safe margin exists for permitting treatment interruptions. The results suggest that the amount of pre-existing impairment (or collagenation) *is directly related* to the *amount* of damage caused by the interruption. Findings also indicate a marked impact on collagen increase of the kinetics of spread (spatial vs random). As such, this may provide direction for further clinical investigation allowing interruptions in a controlled manner, depending on disease progression for individual patients.

Major limitations of the model are clear and include the lack of specific data on FRC and collagen tissue dynamics during interruptions of antiretroviral therapy. The sparseness of sufficiently detailed clinical data is a general issue in the area of biomedical modelling, possibly linked to cost and potential data protection issues involved for open data. However, initiatives like for the Amsterdam Cohort Study on HIV/AIDS, (Coutinho, 1998), fuel the hope of an increasing availability of publicly available data of high quality. Other limitations concern CD4 + movement, where some studies report deviations from the random walk assumed for this model, (Banigan et al., 2015). Also, obtaining sufficiently detailed data to discriminate between clustered and random collagenation might be challenging due to inter-patient variations and assay techniques available.

In addition, FRC dynamics were included indirectly only, to reduce model complexity. This trade-off in depth versus breadth is inevitable to some extent in modelling, but while more extensive models (such as C-IMMSIM) are obviously desirable, practical limitations of data availability for comprehensive and suitably precise parameter estimation as well as high computational expense inevitably apply. The aim here has been to explore lacunae in available model features with the precision achievable, whilst balancing other complexities, in order to address questions such as impact of treatment interruption.

Further efforts must include an additional exploration of the model parameter space including a more detailed sensitivity

analysis to determine the parameters critical for the model. The clinical data available were used as a basis for the inverse Monte Carlo approach, (Mosegaard and Sambridge, 2002). Parameter estimates obtained require both sensitivity analysis and, if possible, further clinical validation especially with regard to small-world properties of the network. Further efforts should also adress the impact of a 3D lattice layout against the 2D layout assumed for this study to rule out the formation of artifacts. Also, exploring differing rates for CD4 + depletion reflecting a whole population as well as regeneration capabilities of collagenated sites, are important aspects motivating future research. Questions clearly remain on the influence of duration, frequency and repetition of interruptions on long-term tissue damage and the possible influence of pharmacological aspects, (Moreno-Gamez et al., 2015). In consequence, our simulations represent a first step, with larger numerical experiments needed to explore the maximum number of interruptions and interruption intervals permissible to maintain appropriate treatment integrity for various degrees of immune system impairment to determine extent and probability of adverse effects, or possible regeneration.

In summary, our study offers a novel view of spatial aspects of collagen formation, which have been neglected in previous studies. In terms of HIV treatment interruptions and their cumulative effects, the approach has the potential to provide guidance in promotion of more flexible treatment options.

Conflict of interest

The authors declare that the research was conducted in the absence of any commercial or financial relationships that could be construed as a potential conflict of interest.

Author contributions

A.H. designed the model and the computational framework, analyzed the data and wrote the manuscript with input from all authors. M.C. and H.R. supervised the project. All authors provided critical feedback and helped shape the research, analysis and manuscript.

Funding

The authors received no specific funding for this work.

CRediT authorship contribution statement

Andreas Hillmann: Conceptualization, Methodology, Software, Investigation, Visualization, Writing - original draft. **Martin Crane:** Supervision, Writing - review & editing, Resources. **Heather J. Ruskin:** Supervision, Writing - review & editing.

Acknowledgment

Access to the Irish Centre for High-End Computing (ICHEC) computational resources is gratefully acknowledged. We thank the two anonymous reviewers whose comments helped improve and clarify this manuscript.

Data availability statement

The program code and simulation data used to support the findings of this study are available from the corresponding author upon request.

References

Ager, A., 2017. High endothelial venules and other blood vessels: Critical regulators of lymphoid organ development and function. Front. Immunol. 8, 1–16. https://doi.org/10.3389/fimmu.2017.00045.

Ager, A., May, M.J., 2015. Understanding high endothelial venules: Lessons for cancer immunology. Oncoimmunology 4,. https://doi.org/10.1080/2162402X.2015.1008791 e1008791.

Appay, V., Sauce, D., 2017. Assessing immune aging in HIV-infected patients. Virulence 8, 529–538. https://doi.org/10.1080/21505594.2016.1195536.

Banigan, E.J., Harris, T.H., Christian, D.A., Hunter, C.A., Liu, A.J., 2015. Heterogeneous CD8+ T cell migration in the lymph node in the absence of inflammation revealed by quantitative migration analysis. PLOS Comput. Biol. 11. https://doi.org/10.1371/journal.pcbi.1004058 e1004058.

Beauchemin, C., Forrest, S., Koster, F.T., 2006. Modeling influenza viral dynamics in tissue. Artif. Immune Syst., 23–36 https://doi.org/10.1007/11823940_3.

Beltman, J.B., Marée, A.F.M., Lynch, J.N., Miller, M.J., de Boer, R.J., 2007. Lymph node topology dictates T cell migration behavior. J. Exp. Med. 204, 771–780. https://doi.org/10.1084/jem.20061278.

Benson, C.A., 2006. Structured treatment interruptions–new findings. Top. HIV Med. 14, 107–111.

Bernaschi, M., Castiglione, F., 2001. Design and implementation of an immune system simulator. Comput. Biol. Med. 31, 303–331. https://doi.org/10.1016/S0010-4825(01)00011-7.

Bocharov, G., Novkovic, M., Onder, L., Kislitsyn, A., Savinkov, R., 2015. Modelling the FRC network of lymph node, in, Int. Work. Artif. Immune Syst. IEEE 2015, 1–2. https://doi.org/10.1109/AISW.2015.7469235.

Bogle, G., Dunbar, P.R., 2010. Agent-based simulation of T-cell activation and proliferation within a lymph node. Immunol. Cell Biol. 88, 172–179. https://doi.org/10.1038/icb.2009.78.

Brenner, B.G., Routy, J.-P., Petrella, M., Moisi, D., Oliveira, M., Detorio, M., Spira, B., Essabag, V., Conway, B., Lalonde, R., Sekaly, R.-P., Wainberg, M.A., 2002. Persistence and fitness of multidrug-resistant human immunodeficiency Virus Type 1 acquired in primary infection. J. Virol. 76, 1753–1761. https://doi.org/10.1128/JVI.76.4.1753-1761.2002.

Bueno-Orovio, A., Hermans, A.N., Greig, R.J.H., Britton, O.J., Passini, E., Lu, H.R., Rohrbacher, J., Gallacher, D.J., Rodriguez, B., 2017. Human in silico drug trials demonstrate higher accuracy than animal models in predicting clinical pro-arrhythmic cardiotoxicity. Front. Physiol. 8, 1–15. https://doi.org/10.3389/fphys.2017.00668.

Castiglione, F., Celada, F., 2015. Immune system modelling and simulation. CRC Press. https://doi.org/10.1201/b18274.

Castiglione, F., Pappalardo, F., Bernaschi, M., Motta, S., 2007. Optimization of HAART with genetic algorithms and agent-based models of HIV infection. Bioinformatics 23, 3350–3355. https://doi.org/10.1093/bioinformatics/btm408.

Celada, F., Seiden, P.E., 1992. A computer model of cellular interactions in the immune system. Immunol. Today 13, 56–62. https://doi.org/10.1016/0167-5699(92)90135-T.

Chavali, A.K., Gianchandani, E.P., Tung, K.S., Lawrence, M.B., Peirce, S.M., Papin, J.A., 2008. Characterizing emergent properties of immunological systems with multi-cellular rule-based computational modeling. Trends Immunol. 29, 589–599. https://doi.org/10.1016/j.it.2008.08.006.

Coutinho, R.A., 1998. The amsterdam cohort studies on HIV infection and AIDS. J. Acquir. Immune Defic. Syndr. Hum. Retrovirol. 17, S4–S8. https://doi.org/10.1097/00042560-199801001-00003.

Donovan, G.M., Lythe, G., 2012. T-cell movement on the reticular network. J. Theor. Biol. 295, 59–67. https://doi.org/10.1016/j.jtbi.2011.11.001.

Donovan, G.M., Lythe, G., 2016. T cell and reticular network co-dependence in HIV infection. J. Theor. Biol. 395, 211–220. https://doi.org/10.1016/j.jtbi.2016.01.040.

El-Sadr, W.M., Lundgren, J.D., Neaton, J.D., Gordin, F., Abrams, D., Arduino, R.C., Babiker, A., Burman, W., Clumeck, N., Cohen, C.J., Cohn, D., Cooper, D., Darbyshire, J., Emery, S., Fätkenheuer, G., Gazzard, B., Grund, B., Hoy, J., Klingman, K., Losso, M., Markowitz, N., Neuhaus, J., Phillips, A., Rappoport, C., 2006. CD4+ count-guided interruption of antiretroviral treatment. N. Engl. J. Med. 355, 2283–2296. https://doi.org/10.1056/NEJMoa062360.

Escobar Ospina, M.E., Perdomo, J.G., 2013. A growth model of human papillomavirus type 16 designed from cellular automata and agent-based models. Artif. Intell. Med. 57, 31–47. https://doi.org/10.1016/j.artmed.2012.11.001.

Estes, J.D., 2013. Pathobiology of HIV/SIV-associated changes in secondary lymphoid tissues. Immunol. Rev. 254, 65–77. https://doi.org/10.1111/imr.12070.

Estes, J.D., Reilly, C., Trubey, C.M., Fletcher, C.V., Cory, T.J., Piatak, M., Russ, S., Anderson, J., Reimann, T.G., Star, R., Smith, A., Tracy, R.P., Berglund, A., Schmidt, T., Coalter, V., Chertova, E., Smedley, J., Haase, A.T., Lifson, J.D., Schacker, T.W., 2015. Antifibrotic therapy in simian immunodeficiency virus infection preserves CD4+ T-Cell populations and improves immune reconstitution with antiretroviral therapy. J. Infect. Dis. 211, 744–754. https://doi.org/10.1093/infdis/jiu519.

Fauci, A.S., Pantaleo, G., Stanley, S., Weissman, D., 1996. Immunopathogenic mechanisms of HIV infection. Ann. Intern. Med. 124, 654–663. https://doi.org/10.1016/0090-1229(89)90122-0.

Fletcher, A.L., Acton, S.E., Knoblich, K., 2015. Lymph node fibroblastic reticular cells in health and disease. Nat. Rev. Immunol. 15, 350–361. https://doi.org/10.1038/nri3846.

Ganeshalingam, S., Koh, D.-M., 2009. Nodal staging. Cancer Imag. 9, 104–111. https://doi.org/10.1102/1470-7330.2009.0017.
Ganusov, V.V., Auerbach, J., 2014. Mathematical modeling reveals kinetics of lymphocyte recirculation in the whole organism. PLoS Comput. Biol. 10. https://doi.org/10.1371/journal.pcbi.1003586.
García, F., Plana, M., Ortiz, G.M., Bonhoeffer, S., Soriano, A., Vidal, C., Cruceta, A., Arnedo, M., Gil, C., Pantaleo, G., Pumarola, T., Gallart, T., Nixon, D.F., Miró, J.M., Gatell, J.M., 2001. The virological and immunological consequences of structured treatment interruptions in chronic HIV-1 infection. AIDS 15, F29–F40. https://doi.org/10.1097/00002030-200106150-00002.
Glass, T., Cavassini, M., 2014. Asking about adherence – From flipping the coin to strong evidence. Swiss Med Wkly., 1–7 https://doi.org/10.4414/smw.2014.14016.
González, R.E.R., De Figueirêdo, P.H., Coutinho, S., 2013. Cellular automata approach for the dynamics of HIV infection under antiretroviral therapies: The role of the virus diffusion. Phys. A Stat. Mech. Its Appl. 392, 4717–4725. https://doi.org/10.1016/j.physa.2012.10.036.
Graw, F., Perelson, A.S., 2013. Spatial Aspects of HIV Infection. In: Ledzewicz, U., Schättler, H., Friedman, A., Kashdan, E. (Eds.), Math. Methods Model. Biomed.. Springer New York, New York, NY, pp. 3–31. https://doi.org/10.1007/978-1-4614-4178-6_1.
Graw, F., Regoes, R.R., 2012. Influence of the fibroblastic reticular network on cell-cell interactions in lymphoid organs. PLoS Comput. Biol. 8,. https://doi.org/10.1371/journal.pcbi.1002436 e1002436.
Greenough, T.C., Brettler, D.B., Kirchhoff, F., Alexander, L., Desrosiers, R.C., O'Brien, S. J., Somasundaran, M., Luzuriaga, K., Sullivan, J.L., 1999. Long-term nonprogressive infection with human immunodeficiency virus type 1 in a Hemophilia Cohort. J. Infect. Dis. 180, 1790–1802. https://doi.org/10.1086/315128.
Günthard, H.F., Aberg, J.A., Eron, J.J., Hoy, J.F., Telenti, A., Benson, C.A., Burger, D.M., Cahn, P., Gallant, J.E., Glesby, M.J., Reiss, P., Saag, M.S., Thomas, D.L., Jacobsen, D. M., Volberding, P.A., nthard 2014. Antiretroviral treatment of adult HIV infection. JAMA 312, 410. https://doi.org/10.1001/jama.2014.8722.
Halling-Brown, M., Pappalardo, F., Rapin, N., Zhang, P., Alemani, D., Emerson, A., Castiglione, F., Duroux, P., Pennisi, M., Miotto, O., Churchill, D., Rossi, E., Moss, D. S., Sansom, C.E., Bernaschi, M., Lefranc, M.-P., Brunak, S., Lund, O., Motta, S., Lollini, P.-L., Murgo, A., Palladini, A., Basford, K.E., Brusic, V., Shepherd, A.J., 2010. ImmunoGrid: Towards agent-based simulations of the human immune system at a natural scale. Philos. Trans. A. Math. Phys. Eng. Sci. 368, 2799–2815. https://doi.org/10.1098/rsta.2010.0067.
Hasenkrug, K.J., Chougnet, C.A., Dittmer, U., 2018. Regulatory T cells in retroviral infections. PLOS Pathog. 14,. https://doi.org/10.1371/journal.ppat.1006776 e1006776.
Hillmann, A., Crane, M., Ruskin, H.J., 2017. HIV models for treatment interruption: Adaptation and comparison. Phys. A Stat. Mech. Appl. 483, 44–56. https://doi.org/10.1016/j.physa.2017.05.005.
A. Hillmann, M. Crane, H.J. Ruskin, A computational lymph tissue model for long term HIV infection progression and immune fitness, in: J. McAuley, S. McKeever (Eds.), Irish Conf. Artif. Intell. Cogn. Sci., Dublin, 2017. http://ceur-ws.org/Vol-2086/AICS2017_paper_13.pdf.
Hirschel, B., Flanigan, T., 2009. Is it smart to continue to study treatment interruptions?. AIDS 23, 757–759. https://doi.org/10.1097/QAD.0b013e328321b791.
Kassutto, S., Maghsoudi, K., Johnston, M.N., Robbins, G.K., Burgett, N.C., Sax, P.E., Cohen, D., Pae, E., Davis, B., Zachary, K., Basgoz, N., D'Agata, M., DeGruttola, E.V., Walker, B.D., Rosenberg, E.S., 2006. Longitudinal analysis of clinical markers following antiretroviral therapy initiated during acute or early HIV type 1 infection. Clin. Infect Dis. 42, 1024–1031. https://doi.org/10.1086/500410.
Linderman, J.J., Riggs, T., Pande, M., Miller, M., Marino, S., Kirschner, D.E., 2010. Characterizing the dynamics of CD4+ T cell priming within a lymph node. J. Immunol. 184, 2873–2885. https://doi.org/10.4049/jimmunol.0903117.
Maggiolo, F., Airoldi, M., Callegaro, A., Martinelli, C., Dolara, A., Bini, T., Gregis, G., Quinzan, G., Ripamonti, D., Ravasio, V., Suter, F., 2009. CD4 cell-guided scheduled treatment interruptions in HIV-infected patients with sustained immunologic response to HAART. AIDS. 27, 799–807. https://doi.org/10.1097/QAD.0b013e328321b75e.
Mancini, E., Castiglione, F., Bernaschi, M., de Luca, A., Sloot, P.M.A., 2012. HIV reservoirs and immune surveillance evasion cause the failure of structured treatment interruptions: A computational study. PLoS One 7,. https://doi.org/10.1371/journal.pone.0036108 e36108.
Mann, M., Lurie, M.N., Kimaiyo, S., Kantor, R., 2013. Effects of political conflict-induced treatment interruptions on HIV drug resistance. AIDS Rev. 15, 15–24.
Masenyetse, L.J., Manda, S., Mwambi, H.G., 2015. An assessment of adverse drug reactions among HIV positive patients receiving antiretroviral treatment in South Africa. AIDS Res. Ther. 12, 6. https://doi.org/10.1186/s12981-015-0044-0.
McGreevy, R.L., 2001. Reverse Monte Carlo modelling. J. Phys. Condens. Matter. 13, R877–R913. https://doi.org/10.1088/0953-8984/13/46/201.
Moreno-Gamez, S., Hill, A.L., Rosenbloom, D.I.S., Petrov, D.A., Nowak, M.A., Pennings, P.S., 2015. Imperfect drug penetration leads to spatial monotherapy and rapid evolution of multidrug resistance. Proc. Natl. Acad. Sci. 112, E2874–E2883. https://doi.org/10.1073/pnas.1424184112.
Mosegaard, K., Sambridge, M., 2002. Monte Carlo analysis of inverse problems. Inverse Probl. 18, R29–R54. https://doi.org/10.1088/0266-5611/18/3/201.
Murray, L.K., Semrau, K., McCurley, E., Thea, D.M., Scott, N., Mwiya, M., Kankasa, C., Bass, J., Bolton, P., 2009. Barriers to acceptance and adherence of antiretroviral therapy in urban Zambian women: A qualitative study. AIDS Care. 21, 78–86. https://doi.org/10.1080/09540120802032643.
Novkovic, M., Onder, L., Cupovic, J., Abe, J., Bomze, D., Cremasco, V., Scandella, E., Stein, J.V., Bocharov, G., Turley, S.J., Ludewig, B., 2016. Topological small-world organization of the fibroblastic reticular cell network determines lymph node functionality. PLoS Biol. 14,. https://doi.org/10.1371/journal.pbio.1002515 e1002515.
Novkovic, M., Onder, L., Cheng, H.-W., Bocharov, G., Ludewig, B., 2018. Integrative computational modeling of the lymph node stromal cell landscape. Front. Immunol. 9, 1–9. https://doi.org/10.3389/fimmu.2018.02428.
Nozaki, I., Kuriyama, M., Manyepa, P., Zyambo, M.K., Kakimoto, K., Bärnighausen, T., 2013. False beliefs about ART effectiveness, side effects and the consequences of non-retention and non-adherence among ART patients in livingstone, Zambia. AIDS Behav. 17, 122–126. https://doi.org/10.1007/s10461-012-0221-2.
Okoye, A.A., Picker, L.J., 2013. CD4+ T-Cell depletion In Hiv infection: Mechanisms of immunological failure. Immunol. Rev. 254, 54–64. https://doi.org/10.1111/imr.12066.
Paci, P., Martini, F., Bernaschi, M., D'Offizi, G., Castiglione, F., 2011. Timely HAART initiation may pave the way for a better viral control. BMC Infect. Dis. 11, 56. https://doi.org/10.1186/1471-2334-11-56.
Pai, N.P., Lawrence, J., Reingold, A.L., Tulsky, J.P., 2006. Structured treatment interruptions (STI) in chronic unsuppressed HIV infection in adults. Cochrane Database Syst. Rev. 3, CD006148. https://doi.org/10.1002/14651858.CD005482.
Pantaleo, G., Graziosi, C., Demarest, J.F., Butini, L., Montroni, M., Fox, C.H., Orenstein, J.M., Kotler, D.P., Fauci, A.S., 1993. HIV infection is active and progressive in lymphoid tissue during the clinically latent stage of disease. Nature 362, 355–358. https://doi.org/10.1038/362355a0.
Perelson, A.S., Nelson, P.W., 1999. Mathematical analysis of HIV-1 dynamics in vivo. SIAM Rev. 41, 3–44. https://doi.org/10.1137/S0036144598335107.
Precharattana, M., 2016. Stochastic modeling for dynamics of HIV-1 infection using cellular automata: A review. J. Bioinform. Comput. Biol. 14, 1630001. https://doi.org/10.1142/S021972001630001X.
C.P. Robert, The Metropolis-Hastings Algorithm, in: Wiley StatsRef Stat. Ref. Online, John Wiley & Sons, Ltd, Chichester, UK, 2015: pp. 1–15. https://doi.org/10.1002/9781118445112.stat07834.
Rosenberg, E.S., Altfeld, M., Poon, S.H., Phillips, M.N., Wilkes, B.M., Eldridge, R.L., Robbins, G.K., D'Aquila, R.T., Goulder, P.J., Walker, B.D., 2000. Immune control of HIV-1 after early treatment of acute infection. Nature 407, 523–526. https://doi.org/10.1038/35035103.
Rothenberger, M.K., Keele, B.F., Wietgrefe, S.W., Fletcher, C.V., Beilman, G.J., Chipman, J.G., Khoruts, A., Estes, J.D., Anderson, J., Callisto, S.P., Schmidt, T.E., Thorkelson, A., Reilly, C., Perkey, K., Reimann, T.G., Utay, N.S., 2015. Large number of rebounding/founder HIV variants emerge from multifocal infection in lymphatic tissues after treatment interruption. Proc. Natl. Acad. Sci. 112, 1–9. https://doi.org/10.1073/pnas.1414926112.
Ruffault, A., Michelet, C., Jacquelinet, C., Guist'hau, O., Genetet, N., Bariou, C., Colimon, R., Cartier, F., 1995. The prognostic value of plasma viremia in HIV-infected patients under AZT treatment: A two-year follow-up study. J. Acquir. Immune Defic. Syndr. Hum. Retrovirol. 9, 243–248. https://doi.org/10.1097/00042560-199507000-00004.
Savinkov, R., Kislitsyn, A., Watson, D.J., van Loon, R., Sazonov, I., Novkovic, M., Onder, L., Bocharov, G., 2017. Data-driven modelling of the FRC network for studying the fluid flow in the conduit system. Eng. Appl. Artif. Intell. 62, 341–349. https://doi.org/10.1016/j.engappai.2016.10.007.
Schacker, T.W., Reilly, C., Beilman, G.J., Taylor, J., Skarda, D., Krason, D., Larson, M., Haase, A.T., 2005. Amount of lymphatic tissue fibrosis in HIV infection predicts magnitude of HAART-associated change in peripheral CD4 cell count. AIDS 19, 2169–2171. https://doi.org/10.1097/01.aids.0000194801.51422.03.
Shen, H., Wang, X., Shao, Z., Liu, K., Xia, X.-Y., Zhang, H.-Z., Song, K., Song, Y., Shang, Z.-J., 2014. Alterations of high endothelial venules in primary and metastatic tumors are correlated with lymph node metastasis of oral and pharyngeal carcinoma. Cancer Biol. Ther. 15, 342–349. https://doi.org/10.4161/cbt.27328.
Spiegel, H., Herbst, H., Niedobitek, G., Foss, H.D., Stein, H., 1992. Follicular dendritic cells are a major reservoir for human immunodeficiency virus type 1 in lymphoid tissues facilitating infection of CD4+ T-helper cells. Am. J. Pathol. 140, 15–22.
Strain, M.C., Richman, D.D., Wong, J.K., Levine, H., 2002. Spatiotemporal dynamics of HIV propagation. J. Theor. Biol. 218, 85–96. https://doi.org/10.1006/yjtbi.3055.
Textor, J., Mandl, J.N., de Boer, R.J., 2016. The reticular cell network: A robust backbone for immune responses. PLoS Biol. 14,. https://doi.org/10.1371/journal.pbio.2000827 e2000827.
Theron, A.J., Anderson, R., Rossouw, T.M., Steel, H.C., 2017. The role of transforming growth factor beta-1 in the progression of HIV/AIDS and development of Non-AIDS-defining fibrotic disorders. Front. Immunol. 8. https://doi.org/10.3389/fimmu.2017.01461.
van den Brekel, M.W., Castelijns, J.A., Snow, G.B., 1998. The size of lymph nodes in the neck on sonograms as a radiologic criterion for metastasis: How reliable is it?. AJNR. Am. J. Neuroradiol. 19, 695–700. http://www.ncbi.nlm.nih.gov/pubmed/9576657.
von Andrian, U.H., Mempel, T.R., 2003. Homing and cellular traffic in lymph nodes. Nat. Rev. Immunol. 3, 867–878. https://doi.org/10.1038/nri1222.
Wakode, A.N., 2013. Drug holidays- new weapon or just a break. Asian J. Biomed. Pharm. Sci. 3, 32–43.
Ward, J.M., Cherian, S., Linden, M.A., 2018. Hematopoietic and Lymphoid Tissues, in. Comp. Anat. Histol., Elsevier, 365–401. https://doi.org/10.1016/B978-0-12-802900-8.00019-1.

WHO, Consolidated guidelines on the use of antiretroviral drugs for treating and preventing HIV infection, (2013) 94-95,109,32-33,90,146-153. http://www.who.int/hiv/pub/guidelines/arv2013/download/en/ (accessed October 28, 2014).

X.-S. Yang, Y.Z.L. Yang, Cellular Automata Networks, in: A. Adamatzky, L. Bull, B. De Lacy Costello, S. Stepney, C. Teuscher (Eds.), Proc. Unconv. Comput. 2007, Luniver Press, 2007: pp. 280–302. http://arxiv.org/abs/1003.4958.

Zeng, M., Smith, A.J., Wietgrefe, S.W., Southern, P.J., Schacker, T.W., Reilly, C.S., Estes, J.D., Burton, G.F., Silvestri, G., Lifson, J.D., Carlis, J.V., Haase, A.T., 2011. Cumulative mechanisms of lymphoid tissue fibrosis and T cell depletion in HIV-1 and SIV infections. J. Clin. Invest. 121, 998–1008. https://doi.org/10.1172/JCI45157.

Zeng, M., Southern, P.J., Reilly, C.S., Beilman, G.J., Chipman, J.G., Schacker, T.W., Haase, A.T., 2012. Lymphoid tissue damage in HIV-1 infection depletes Naïve T cells and limits T cell reconstitution after antiretroviral therapy. PLoS Pathog. 8,. https://doi.org/10.1371/journal.ppat.1002437 e1002437.

Zeng, M., Haase, A.T., Schacker, T.W., 2012. Lymphoid tissue structure and HIV-1 infection: Life or death for T cells. Trends Immunol. 33, 306–314. https://doi.org/10.1016/j.it.2012.04.002.